Simultaneous degeneracy of the confined 2D hydrogen atom energy levels

J. Phys. B: At. Mol. Opt. Phys. **41** (2008) 205002 (9pp) doi:10.1088/0953-4075/41/20/205002

Simultaneous degeneracy of the confined 2D hydrogen atom energy levels

Lj Stevanović[1] and K D Sen[2]

[1] Department of Physics, Faculty of Sciences and Mathematics, University of Niš, Višegradska 33, 18 000 Niš, Serbia
[2] School of Chemistry, University of Hyderabad, Hyderabad 500 046, India

E-mail: ljstevanovic@junis.ni.ac.yu and sensc@uohyd.ernet.in

Received 10 July 2008, in final form 3 September 2008
Published 1 October 2008
Online at stacks.iop.org/JPhysB/41/205002

Abstract
Using the Numerov–Cooley numerical method, we report several interesting characteristics of the eigenspectrum of 2D hydrogen atom confined inside an impenetrable circular boundary of radius ρ_c. At the confinement radius, ρ_c, exactly equal to the location of the only radial node of the unconfined atom state $(l+2, l)$, the successive pairs of the confined atom states (nl) and $(n+1, l+2)$, where $n \geqslant l+2$, are found to become degenerate. Accurate calculations of static dipole polarizability are reported for several confining radii using the standard second-order perturbation theory.

1. Introduction

The confined hydrogen atom model, originally introduced in physics in order to study the pressure effects on the static polarizability of the hydrogen atom [1], has been subsequently employed in many diverse fields of physics such as astrophysics, condensed matter physics, plasma physics, and atomic and molecular physics. This model has been found to be particularly useful in the study of electronic structure when the spatial confinement effects introduced by environmental influence have to be analysed. In such studies the environmental effects are represented by some artificial volume generated by the neighbouring atoms or molecules. The artificial volume can be of different shapes and sizes depending on the particular system under consideration. For details we refer to the available review articles in the literature [2, 3]. The exciting possibilities of fabrication of nano-structures of a few hundred angstroms in size within the modern semiconductor technology have spurred interest in performing accurate electronic structure calculations under the confined conditions within a D-dimensional space. In these nano-structures, carriers are often confined to reduced dimensions as was demonstrated in GaAs–AlGaAs [4–6]. This introduces the specific need for treating the confined systems in two dimensions (2D) in addition to the confined quantum systems in 3D. Several other experimental studies can be listed where the model of the 2D confined system could be applied in principle. For example, the structures produced by ultrathin film growth are inherently in 2D and these are known to exhibit interesting quantum phenomena [7, 8]. The metal adsorption on the Si surface results in the formation of reconstructed 2D layers [9]. Other examples include the thermal compression of 2D atomic hydrogen gas at a small 'cold spot' on the surface of superfluid helium [10] and the structural transformation process of the Ag/SiC surface phase upon atomic hydrogen exposure [11]. To our knowledge, satisfactory models which reproduce the experimental data cited above are as yet unknown.

In this paper, we investigate the non-relativistic 2D hydrogen atom centrally confined in a circular region with impenetrable boundary. It can serve as a model of a quantum dot with the form of circle in the plane with a hydrogen impurity located in the centre of the circle. More specific examples where this model can be applied are listed in [12, 13]. Our prime interest is to focus on its energy levels and the systematic or *simultaneous* (*persistent*) degeneracy between the pairs of states when the radius of the confining circle, ρ_c, has a specific value determined by the value of the angular-momentum quantum number of the *unconfined* atom. To our knowledge, the regularity of the eigenspectrum of confined 2D hydrogen atom (2D-CHA) under these conditions is explained using the analytical method for the first time.

In section 2, we introduce the theoretical model and describe the numerical method used. In section 3, our results of the numerical computation are presented with discussion. In section 4, an explanation of the simultaneous degeneracy

based on the symmetry arguments is presented. Finally, the main results obtained in this work are summarized in section 5.

The atomic units are used throughout the paper: $m = e = \hbar = 1$.

2. The model

2.1. Radial Schrödinger equation and boundary condition

The electron in the 2D hydrogen atom centrally enclosed inside the circle of radius ρ_c (confinement radius) moves in a two-dimensional potential of the form

$$V(\rho) = \begin{cases} -\dfrac{1}{\rho}, & \rho < \rho_c \\ \infty, & \rho \geqslant \rho_c. \end{cases} \tag{1}$$

The form of the potential (1) implies that the nucleus of the atom is placed in the centre of the circle in the xy-plane. The axial symmetry of the potential allows the factorization of the wavefunction into the radial and angular parts $\Psi_{nl}(\rho, \varphi) = R_{nl}(\rho)\exp(il\varphi)/\sqrt{2\pi}$, where the angular wavefunction is the eigenfunction of the angular momentum along the symmetry axis (z-axis) with the corresponding eigenvalue l ($l = 0, \pm1, \pm2, \ldots, \pm(n-1)$) and $n (n = 1, 2, \ldots)$ is principal quantum number $n = n_\rho + |l| + 1$, where the radial quantum number $n_\rho (n_\rho = 0, 1, 2, \ldots)$ counts the zeros of the radial wavefunction R_{nl}. The absolute value $|l|$ labels the states of the 2D-CHA, as is the case for the free (unconfined) system [14]. The radial wavefunction is the solution of the radial Schrödinger equation

$$\frac{\mathrm{d}^2 R_{nl}}{\mathrm{d}\rho^2} + \frac{1}{\rho}\frac{\mathrm{d}R_{nl}}{\mathrm{d}\rho} + \left[2E + \frac{2}{\rho} - \frac{l^2}{\rho^2}\right] R_{nl} = 0 \tag{2}$$

with the imposed Dirichlet boundary condition

$$R_{nl}(\rho_c) = 0. \tag{3}$$

The requirement that the radial wavefunction must be finite everywhere leads to the behaviour $R_{nl}(\rho) \sim \rho^l$ in the vicinity of the origin ($\rho = 0$).

Due to the term l^2 in the radial Schrödinger equation (2) it is clear that 2D-CHA energy levels are two-fold degenerated except for the state with $l = 0$. This is the reason why we take only the states with non-negative l values into consideration unless it is indicated otherwise.

A brief account of the notation of the 2D-CHA states is in order. In [13] the 2D-CHA wavefunctions are labelled by the pairs of quantum numbers $(n_\rho\mu)$, where μ is the azimuthal (magnetic) quantum number identical to our $|l|$, and spectroscopic notations of the states are given by small Greek letters (as in the case of diatomic molecules). Alternatively, in [12] the labelling by the pairs $(n|l|)$ is given and spectroscopic notations are the same as in the case of hydrogen atom in 3D (confined and unconfined). We follow the notation as it is accepted for the unconfined 2D hydrogen atom [14] and in [12]. In the graphical illustration, the two notations have been reconciled.

2.2. Numerical method

Solving the eigenvalue problem (2)–(3) needs some of the numerical methods. We will apply the finite difference method of high accuracy, known as the Numerov–Cooley method [15, 16] which is originally developed for solving the eigenvalue problems when the corresponding differential equation does not contain the first-order derivative. If a new function $P_{nl}(\rho) = \sqrt{\rho}R_{nl}(\rho)$ is introduced, the radial Schrödinger equation (2) takes the form

$$\frac{\mathrm{d}^2 P_{nl}}{\mathrm{d}\rho^2} = [U(\rho) - 2E]P_{nl}, \tag{4}$$

where

$$U(\rho) = \frac{l^2 - 1/4}{\rho^2} - \frac{2}{\rho} \tag{5}$$

and the conditions imposed on the function P_{nl} are

$$P_{nl}(0) = 0 \qquad \text{and} \qquad P_{nl}(\rho_c) = 0. \tag{6}$$

The difference equation, corresponding to equation (4), is obtained by introducing the grid of n equally spaced points on the interval $[0, \rho_c]$ by step h,

$$\rho_i = (i-1)h, \qquad i = 1, 2 \ldots n \quad (\rho_1 = 0, \rho_n = \rho_c), \tag{7}$$

and takes the form

$$Y_{i+1} - 2Y_i + Y_{i-1} = h^2(U_i - 2E)P_i, \tag{8}$$

where $P_i = P_{nl}(\rho_i)$, $U_i = U(\rho_i)$ and

$$Y_i = \left\{1 - \frac{h^2}{12}(U_i - 2E)\right\} P_i. \tag{9}$$

To start the Numerov–Cooley integration the values for P_1, P_2, P_{n-1} and P_n are needed. Two of them, P_1 and P_n, are known from the boundary conditions (6). For P_{n-1} a small arbitrary number p: $P_{n-1} = p$ is prescribed [16]. Since the origin $\rho = 0$ is the singular point of the radial Schrödinger equation (4) the procedure outlined in [17] is used here: The Fröbenius method [18] can be applied to yield the regular solution in this region through the power series $P_i = \sum_{k=1}^{Q} c_k \rho_i^{k+\alpha}$ in the first M points ($i = 1, 2, 3, \ldots, M$) with $\alpha = |l| - 1/2$ and recurrence relation among the coefficients

$$c_k = \frac{2Ec_{k-2} + 2c_{k-1}}{l^2 - \frac{1}{4} - (k + \alpha - 1)(k + \alpha)}, \tag{10}$$

where $c_1 = 1$ and $c_k = 0$ if $k \leqslant 0$.

Using the recurrence relation (8) with given P_n, P_{n-1} and guessed energy values E_g, inward integration is performed giving $Y_{n-2}, Y_{n-3}, \ldots$ from which then the corresponding P_i^{in} values are calculated according to (9). Similarly, starting with the first M values of P_i and using the recurrence relation (8) outward integration yields $Y_{M+1}, Y_{M+2}, \ldots$, and from them the corresponding P_i^{out} values. Inward and outward integrations are carried out to some matching point ρ_m that is chosen to be an extremum point for the wavefunction [16] and at that point the two sets P_i^{in} and P_i^{out} are scaled so that $P_m^{\text{in}} = P_m^{\text{out}} = 1$. Then, the error function is defined as

$$F(E_g) = Y_{m+1}^{\text{in}} + Y_{m-1}^{\text{out}} - 2Y_m - h^2(U_m - 2E_g)P_m, \tag{11}$$

Table 1. Computed energy values of 2s state of 2D-CHA at confinement radius $\rho_c = 2.0$ for different values of parameters ϵ (accuracy), N, M and E_g. The energy value given in [12] is $E = 1.607\,823\,563\,313\,719$.

ϵ	N	M	E_g	E	Number of iterations
1.0×10^{-10}	20 000	100	1.607 83	1.607 823 580 6	2
1.0×10^{-10}	20 000	80	1.607 83	1.607 823 569 1	2
1.0×10^{-10}	20 000	50	1.607 83	1.607 823 553 9	2
1.0×10^{-10}	50 000	100	1.607 83	1.607 823 562 9	3
1.0×10^{-11}	50 000	100	1.607 83	1.607 823 562 89	4
1.0×10^{-11}	50 000	100	1.607 824	1.607 823 562 88	3
1.0×10^{-12}	60 000	100	1.607 83	1.607 823 562 908	5
1.0×10^{-12}	60 000	100	1.607 824	1.607 823 562 916	3
1.0×10^{-12}	75 000	100	1.607 823 6	1.607 823 562 651	6
1.0×10^{-12}	75 000	80	1.607 824	1.607 823 561 647	4
1.0×10^{-12}	75 000	200	1.607 823 56	1.607 823 564 953	4
1.0×10^{-13}	80 000	100	1.607 823 563	1.607 823 563 266 3	3
1.0×10^{-13}	80 000	200	1.607 823 563	1.607 823 564 986 9	4
1.0×10^{-14}	80 000	100	1.607 823 563	1.607 823 563 266 31	3
1.0×10^{-14}	80 000	100	1.607 823 563 3	1.607 823 563 269 28	2
1.0×10^{-15}	80 000	100	1.607 823 563 3	1.607 823 563 269 281	3

and the eigenvalues E are determined as the error function zeros by the iterative procedure correcting it in each iteration by the amount

$$D(E_g) = -\frac{F(E_g)Y_m}{2h^2 \sum_{i=1}^{n} P_i^2}. \tag{12}$$

An iterative algorithm is employed such that the prescribed convergence criterion $|D(E_g)| \leqslant \epsilon$ is met. This convergence criterion defines the numerical accuracy with which the numerical integration is performed [17].

3. Results

3.1. Energy levels and intersections

For performing the Numerov–Cooley integration, the values of the required parameters p, Q, M, h (or number of grid points N), ϵ and E_g have to be given. We have used $p = 1.0 \times 10^{-30}$ according to the explanation given in [17]. Our extended numerical calculations showed that the results changed slightly for $Q = 1, 2, 3$ and they were insensitive to the choice of $Q \geqslant 4$. Therefore we have set $Q = 4$ in the numerical calculations. Concerning the choice of the trial energy value E_g, a preliminary consideration is needed. Since we deal here with the confined central-field system we can use the result from [19] that the energy levels are decreasing monotonic functions of the dimension of the confining box, in our case, of confinement radius which converge smoothly to the corresponding energy levels of the unconfined (free) system. Hence, for large ρ_c values the 2D-CHA energy levels approach the energy levels of the unconfined 2D hydrogen atom and the energies of the states of the former quantum system are very close to the energies of the corresponding states of the later system. When ρ_c is small, the radial distance ρ under the third term inside the square brackets (centrifugal potential energy) in the radial Schrödinger equation (2) dominates over the Coulomb potential energy (the second term) and (2) reduces to the radial Schrödinger equation for the infinite potential well in 2D. Here, the energy spectrum is given by the zeros of the equation

$$J_l(\rho_c\sqrt{2E_{nl}}) = 0, \tag{13}$$

where J_l is a Bessel function of the first kind [20]. Hence, the trial energy value E_g is given by the zero of the equation (13) for a small confinement radius [20], and by the energy eigenvalue of the unconfined 2D hydrogen atom for large ρ_c [14]. At the intermediate ρ_c values we use the solutions of the equation (13) for the first run of our numerical code, and then the results obtained in this way are used as input parameters for the second run.

With properly chosen E_g only a few iterations are needed to get the energy value with given accuracy ϵ while the change in other parameters' values, M and N, slightly modifies the energy values. This is demonstrated by the results in table 1 for the 2s state at the confinement radius $\rho_c = 2.0$, obtained with different numerical accuracies. The difference between our value, computed with the highest accuracy $\epsilon = 1.0 \times 10^{-15}$, and the one from [12] is $\Delta E = 4.4438 \times 10^{-11}$.

In our numerical code the counting of zeros of the radial wavefunction is included so as to facilitate the correct identification of the state. Along with the computation of eigenenergies we have calculated the radial wavefunction values at the grid points and used it to calculate the mean values of the radial distance and its square in the ground state. The excellent quantitative agreement is found with the data available in the literature [12] which is displayed in table 2. Thus, not only the eigenspectrum, but also the other properties of the 2D-CHA, like the mean values of ρ and ρ^2 and electric dipole polarizability (that is the subject of subsection 3.3) are obtained with high numerical accuracy by the presently chosen numerical method.

Table 3 contains the energy values of the first few states with $l = 0 - 3$. They are obtained with $M = 100 - 500$ and $N = 80\,000$ for small confinement radius values to $N = 150\,000$ for large values of confinement radius and with accuracy $\epsilon = 1.0 \times 10^{-12}$, but are reported with eight decimal digits in order to save the space. The excellent match with

Table 2. Computed mean values of the radial coordinate and its square in the ground state of 2D-CHA for different ρ_c values, compared with the data from [12].

	$\overline{\rho}$		$\overline{\rho}^2$	
ρ_c	This work	[12]	This work	[12]
0.5	0.192 088 0533	0.192 088 0531	0.046 412 7893	0.046 412 7892
1.0	0.336 824 5426	0.336 824 5420	0.149 285 0948	0.149 285 0945
2.0	0.474 529 5650	0.474 529 5650	0.323 606 2030	0.323 606 2033
4.0	0.499 908 5584	0.499 908 5593	0.374 697 1534	0.374 697 1558
8.0	0.499 999 9888	0.500 000 0000	0.374 999 9808	0.374 999 9994

Table 3. Energies of some 2D-CHA states at different values of the confinement radius.

ρ_c	1s	2s	3s	4s
0.1	253.457 939 40	1479.806 236 47	3696.147 203 88	6900.737 758 64
0.2	54.140 500 75	358.926 999 62	911.941 811 84	1712.337 241 32
0.5	3.907 318 37	52.069 123 91	140.069 550 84	267.784 493 47
1.0	−1.349 785 72	10.758 194 35	32.566 288 94	64.354 899 32
2.0	−1.981 158 59	1.607 823 56	6.926 035 66	14.795 274 39
3.0	−1.999 464 54	0.298 542 27	2.563 615 66	6.013 060 46
4.0	−1.999 986 57	−0.038 145 69	1.173 807 76	3.078 346 16
5.0	−1.999 999 69	−0.150 155 42	0.592 696 61	1.785 149 64
6.0	−1.999 999 99	−0.192 827 80	0.308 879 86	1.117 790 07
8.0	−2.000 000 00	−0.217 363 86	0.067 261 03	0.501 045 97
∞	−2.000 000 00	−0.222 222 22	−0.080 000 00	−0.040 816 33
ρ_c	2p	3p	4p	5p
0.1	713.516 765 80	2434.638 288 35	5145.075 733 78	8843.490 107 58
0.2	173.212 691 16	602.074 693 33	1278.785 089 62	2202.728 317 21
0.5	25.213 211 09	93.158 029 66	201.004 227 84	348.520 517 80
1.0	5.242 787 51	21.956 117 52	48.742 993 57	85.492 913 89
2.0	0.760 782 85	4.812 348 44	11.425 003 02	20.549 668 32
3.0	0.079 817 16	1.832 574 17	4.736 014 46	8.764 457 37
4.0	−0.110 082 29	0.855 960 17	2.469 991 24	4.721 261 37
5.0	−0.177 291 11	0.434 731 86	1.455 715 31	2.887 290 82
6.0	−0.203 804 14	0.223 008 48	0.923 609 49	1.911 394 29
8.0	−0.219 239 25	0.037 212 32	0.421 045 61	0.969 380 94
∞	−0.222 222 22	−0.080 000 00	−0.040 816 33	−0.024 691 36
ρ_c	3d	4d	4f	5f
0.1	1301.491 686 07	3520.810 667 76	2019.644 190 18	4744.495 472 32
0.2	321.057 171 85	874.775 217 01	500.988 695 28	1181.275 517 96
0.5	49.291 770 71	137.353 915 07	78.272 965 48	186.674 407 18
1.0	11.452 382 52	33.246 782 71	18.780 615 37	45.695 834 52
2.0	2.422 863 28	7.761 916 32	4.299 290 19	10.935 611 72
3.0	0.877 984 21	3.203 035 80	1.733 582 15	8.672 380 50
4.0	0.380 035 03	1.661 598 23	0.874 698 01	2.487 722 24
5.0	0.168 963 84	0.972 896 63	0.495 008 22	1.512 707 05
6.0	0.064 680 89	0.612 169 09	0.298 376 24	0.995 017 07
8.0	0.024 978 54	0.272 004 59	0.116 086 61	0.496 756 12
∞	−0.080 000 00	−0.040 816 33	−0.040 816 33	−0.024 691 36

the results presented in table 1 of [12] is obvious for all the common states. Due to that fact in the rest of the paper we will report the results obtained with $n = 50.000$ for all confinement radius values and $\epsilon = 1.0 \times 10^{-5}$ (5 decimal digits) and the given accuracy is enough to make the relevant conclusions. Table 3 and figure 1 show that the energy values of the (nl) states of the 2D-CHA decrease monotonically to the values of the same unconfined 2D hydrogen atom states with increasing confinement radius and they are given in the last rows of table 3 ($\rho_c = \infty$).

The Coulomb degeneracy, a characteristic of the unconfined 2D hydrogen atom, is removed in the confined atom case for all finite ρ_c values. This is expected due to the different boundary condition imposed on the radial wavefunction. The energies of the 2D-CHA states depend differently on the confinement radius as a parameter. Therefore, it is likely that for some ρ_c the states (nl) and $(n'l')$ have the same energies. The numerical results from table 3 and figure 1 show two main features. First, some of these confined states have the energy values matching those

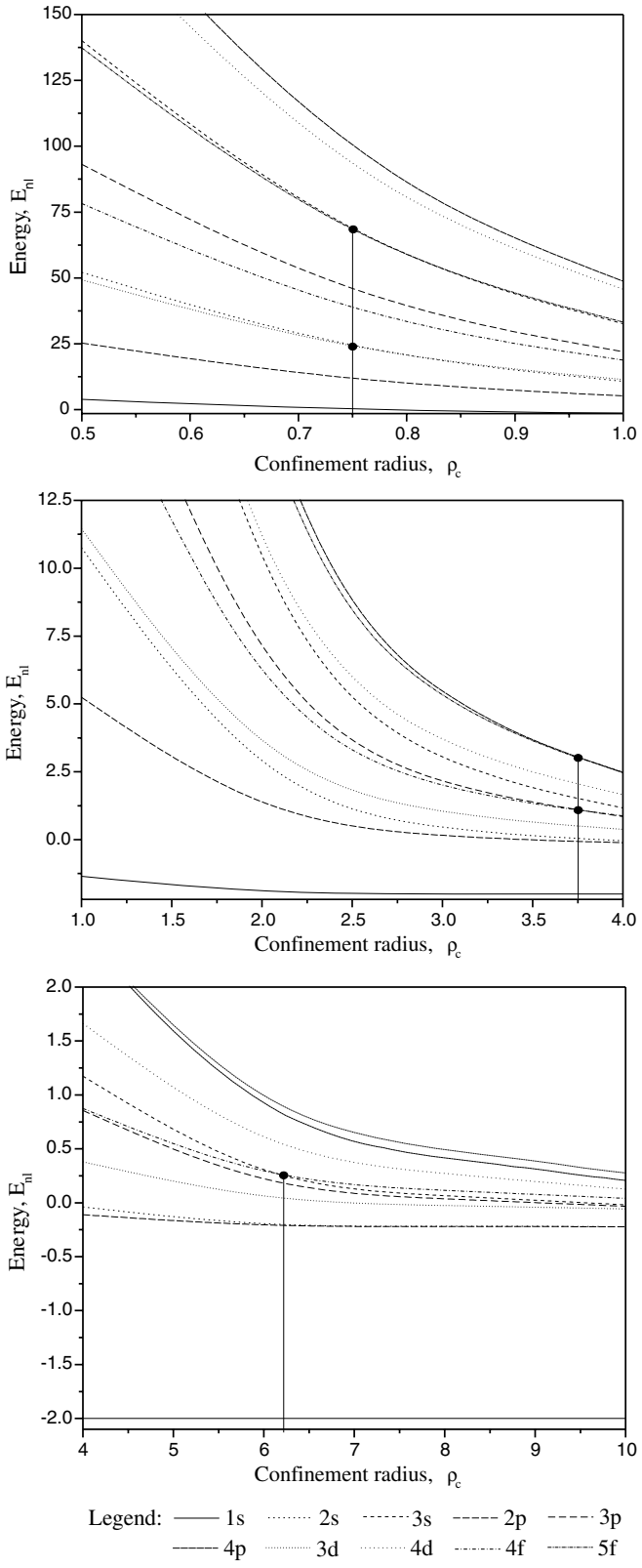

Figure 1. 2D-CHA energy levels versus confinement radius and corresponding intersections.

from the eigenspectrum of the unconfined 2D hydrogen atom. Such unconfined states contain a greater number of radial nodes than the confined state. Such a degeneracy effect is known as *incidental degeneracy*. Incidental degeneracy appears when the confinement radius coincides with the radial wavefunction node of some unconfined 2D hydrogen atom state (nl). In this case there is only one state $(n'l)$ with $n' \neq n$ of 2D-CHA in which energy is given by the same expression as the energy of the (nl) state of unconfined 2D hydrogen atom. The criterion (ρ_c) for this type of degeneracy for the confined system is easily established through the computation of the nodes of the unconfined 2D hydrogen atom radial wavefunctions and it is not of particular interest here, although it will appear later. Secondly, there are 'intersections' between the energy levels, some of them with systematic character when a pair of confined states is defined by the condition $(l' - l) \pm 2$. This effect, known as *simultaneous degeneracy* will now be considered in detail in the following section.

Intersections between the states are easy to be established from their orderings that change from small to large-ρ_c values. As we have already stated, in the small-ρ_c limit the 2D-CHA eigenspectrum can be approximated as the spectrum of the 2D infinite potential well so that the ordering of the states is

$$1s, 2p, 3d, 2s, 4f, 3p, 5g, 4d, 3s, 6h, 5f, \ldots, \qquad (14)$$

as is confirmed by table 3 and figure 1. The procedure similar to that given in [21], when it is applied to our system at large values of ρ_c, draws the conclusion that among the 2D-CHA states with the same quantum number n but different l (these states belong to the same energy level of the unconfined system) the state with a maximal value of $l(l = n - 1)$ is the lowest-laying one on the energy scale. Thus, the ordering of the states in the $\rho_c \to \infty$ limit is given by

$$1s, 2p, 2s, 3d, 3p, 3s, 4f, 4d, 4p, 4s, 5g, 5f, \ldots \qquad (15)$$

The change from (14) to (15) is confirmed by table 3 and figure 1.

The panel on the top of figure 1 proves that the states from the pairs (2s, 3d) and (3s, 4d) have the same energies when $\rho_c = 0.75$. In [12], only the crossing for the 2s and 3d states was reported and the estimation of the confinement radius value at which it takes place $\rho_c \sim 0.8$ was made. In the middle panel of the same figure it can be seen that the intersections between the 3p and 4f states, as well as between the 4p and 5f states appear at the same value of the confinement radius $\rho_c = 3.75$. Our extended numerical calculations show that these intersections have the systematic character and they are the examples of simultaneous degeneracy. This type of degeneracy exhibits itself in the fact that all the states from the pairs $[nl, (n + 1, l + 2)]$ with $n \geqslant l + 2$ have the same energy when ρ_c has a value specified by the quantum number l. Explanation of simultaneous degeneracy and the corresponding ρ_c values at which it appears are given in the following section.

Intersections between the states with $\Delta l \geqslant 2$ are without any systematic character as can be seen in the panel on the bottom of figure 1, where the intersection between (3s, 4f) states is shown. In table 4, we reported some of the pairs of the states between which intersection occurs along with the corresponding ρ_c values at which it happens, as well as their energy in that situation.

Table 4. Intersections between some pairs of the 2D-CHA states.

Pair of states	ρ_c	E
3s 4f	6.196 50	0.271 35
3s 5g	2.583 79	3.739 07
4p 5g	14.672 40	0.029 89
4p 6h	7.935 96	0.431 07
5d 7j	15.140 00	0.123 85

3.2. Static electric dipole polarizability

By definition, the static electric dipole polarizability determines the second-order response of the quantum electronic system to the uniform external static electric field. For the ground state of the unconfined 2D hydrogen atom when the external electric field is applied along the x-axis, it is given by [14]

$$\alpha = \sum_{n=2} \frac{|\langle R_{np}|\rho|R_{1s}\rangle|^2}{E_{np} - E_{1s}} \tag{16}$$

and the same formula is used here for computing the dipole polarizability for 2D-CHA. This is analogous to the case of confined 3D hydrogen atom where the expression for determining α is the same as for the unconfined 3D hydrogen atom (see, for example, [22, 23]). The electric dipole polarizability plays an important role in defining the suitability of the system as a device application (see [24] and references therein). The calculations of α for the 2D-CHA system are therefore of some interest.

In computing the dipole polarizability we keep a different number of terms in (16) for different ρ_c values and omit the terms with contributions equal to or less than 1.0×10^{-7}. The electric dipole polarizability can be calculated in the Kirkwood approximation yielding for our system the result [12]

$$\alpha_K = \overline{\rho^2}. \tag{17}$$

Our results for α_K and those from [12] are almost identical according to the entries in the fourth and fifth columns of table 2. Dipole polarizability is an increasing function of the confinement radius attaining the saturation at large ρ_c values, already at $\rho_c \geqslant 6.0$, as is evident from figure 2 and table 5 when its value coincides with the corresponding value of the unconfined 2D hydrogen atom as it is demonstrated by the last row of table 5.

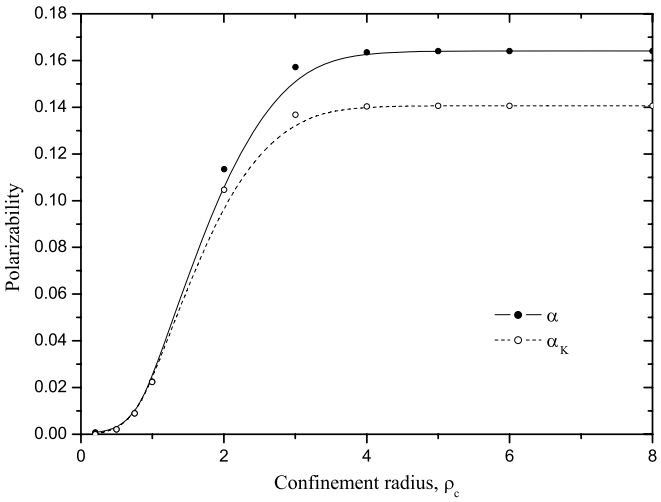

Figure 2. Polarizability of 2D-CHA as a function of the confinement radius.

Table 5. The static electric dipole polarizability for the ground state of 2D-CHA as a function of the confinement radius. The third column contains the Kirkwood polarizability.

ρ_c	α	α_K
0.2	0.000 69	0.000 07
0.5	0.002 18	0.002 15
0.75	0.008 99	0.008 91
1.0	0.022 59	0.022 29
2.0	0.113 39	0.104 72
3.0	0.157 16	0.136 85
4.0	0.163 54	0.140 40
5.0	0.164 03	0.140 61
6.0	0.164 06	0.140 62
8.0	0.164 06	0.140 62
∞	0.164 06	0.140 62

4. Simultaneous (persistent) degeneracy

The energy levels of the unconfined 2D hydrogen atom are characterized by Coulomb degeneracy which results in the states with the same principal quantum number having the same energy [14]

$$E_{nl} = -\frac{1}{2\left(n - \frac{1}{2}\right)^2}. \tag{18}$$

This is the consequence of the existence of the Lenz vector which is an additional integral of motion and its form for the 2D case is [25, 26]

$$\mathbf{A} = \tfrac{1}{2}(\mathbf{p} \times \mathbf{L} - \mathbf{L} \times \mathbf{p}) - \mathbf{e}_\rho, \tag{19}$$

where $\mathbf{p}$ is a momentum-operator, $\mathbf{L}$ is the angular-momentum projection operator ($\mathbf{L} = L\mathbf{e}_z$) and $\mathbf{e}_\rho$ is a unit vector in the ρ-direction. The Lenz vector is not the integral of motion for 2D-CHA since the different boundary condition (3) is imposed on its radial wavefunction. In spite of this fact, in this subsection we will find the operators commuting with the Hamiltonian of 2D-CHA and they will be the squares of the spherical components of the Lenz vector:

$$A_{\pm 1} = A_x \pm \mathrm{i}A_y = \mp\frac{\mathrm{i}}{2}(p_{\pm 1}L + Lp_{\pm 1}) - \frac{x \pm \mathrm{i}y}{\rho}. \tag{20}$$

Their applications on the wavefunction Ψ_{nl} result in

$$A_{\pm 1}^2(R_{nl}\,\mathrm{e}^{\mathrm{i}l\varphi}) = h_{\pm 1}(\rho)\mathrm{e}^{\mathrm{i}(l\pm 2)\varphi}, \tag{21}$$

where

$$h_{\pm 1}(\rho) = \left[\pm 2(l \pm 1) \mp \frac{(l \pm 1)(2l \pm 1)(2l \pm 3)}{2\rho}\right]\frac{\mathrm{d}R_{nl}}{\mathrm{d}\rho} + \left[\frac{l(l \pm 1)(lm \pm 1)(2l \pm 3)}{2\rho^2} - \frac{(l \pm 1)(4l \pm 3)}{\rho} - \frac{E(2l \pm 1)(2l \pm 3)}{2} + 1\right]R_{nl}. \tag{22}$$

The radial function h_{+1} satisfies the Dirichlet boundary condition (3) and, accordingly, it is the radial wavefunction of some 2D-CHA state, only if the confinement radius is

$$\rho_c = \left(l + \tfrac{1}{2}\right)\left(l + \tfrac{3}{2}\right), \tag{23}$$

which is the zero of the radial wavefunction of the unconfined 2D hydrogen atom state with $n_\rho = 1$ and $n = l + 2$ and the same quantum number l as in the 2D-CHA case. An analogous statement is valid for the radial function h_{-1} when the radius of confinement is given by

$$\rho_c = \left(l - \tfrac{1}{2}\right)\left(l - \tfrac{3}{2}\right) \quad (l \neq 1). \tag{24}$$

From (21) and after additional algebraic derivations it can be concluded that h_{+1} and h_{-1} are the solutions of the radial Schrödinger equation (2) with the quantum numbers $l + 2$ and $l - 2$, respectively, and energy E, the same as energy of the 2D-CHA state with the radial wavefunction R_{nl} when the confining radius is given by (23) or (24). Thus, we have $h_{\pm 1} \equiv R_{n',l\pm 2}$ and the remaining task is to find the relation between the principal quantum numbers n and n'. In the following paragraph we will take into account only the operator A^2_{+1} and function h_{+1} and prove that only the curves E_{nl} and $E_{n+1,l+2}$ as the functions of the confinement radius can intersect.

In the $\rho_c \to \infty$ limit, $E_{nl} \to -1/[2(n - 1/2)^2]$ and $E_{n+1,l+2} \to -1/[2(n + 1/2)^2]$ so that $E_{n+1,l+2} < E_{nl}$. In the $\rho_c \to 0$ limit, if we remember the theorems on interlacing the zeros of Bessel functions [20] and the fact that E_{nl} is the $(n - l)$ th solution of the eigenvalue problem (2)–(3), we get $E_{nl} < E_{n+1,l+2}$. Thus, there must be some finite value of the confinement radius at which these curves $E_{nl}(\rho_c)$ and $E_{n+1,l+2}(\rho_c)$ will intersect. To prove that $n' = n + 1$ is the only possibility we will use the following arguments. The differential operators in (2) corresponding to the quantum numbers $l + 2$ and l differ by the positive term $[(l + 2)^2 - l^2]/(2\rho^2)$. Taking into account that $E_{n+2,l+2}$ and E_{nl} are the $(n - l)$ th solutions of the eigenvalue problem (2)–(3) when the angular momentum quantum number has the values $l + 2$ and l, respectively, and using the min–max principle and the corresponding theorems, such as Sturm oscillation theorem, that follow from its application on the bound states of the Schrödinger operators [27], it follows that $E_{nl} < E_{n+2,l+2}$. From the obvious facts this inequality can be expanded to

$$E_{nl} < E_{n+2,l+2} < E_{n+3,l+2} < E_{n+4,l+2} < \cdots, \tag{25}$$

proving that the only possibility for the curves E_{nl} and $E_{n',l+2}$ to intersect in the ρ_c–E plane is $n' = n + 1$.

Hence, we prove that $h_{\pm 1}$ are the radial wavefunctions corresponding to the states with the quantum numbers $n \pm 1$ and $l \pm 2$: $h_{\pm 1} \sim R_{n\pm 1,l\pm 2}$ or

$$\Psi_{nl} \xrightarrow{A^2_{+1}} \Psi_{n+1,l+2} \xrightarrow{A^2_{-1}} \Psi_{nl} \qquad \text{when} \qquad \rho_c = \left(l + \frac{1}{2}\right)\left(l + \frac{3}{2}\right) \qquad \text{and} \qquad n \geqslant l + 2. \tag{26}$$

Operators $A^2_{\pm 1}$ perform mutual transformations among the 2D-CHA states given in the above expression and they perform the role of angular momentum raising $\left(A^2_{+1}\right)$ and lowering $\left(A^2_{-1}\right)$ operators changing it by two units. At the same time,

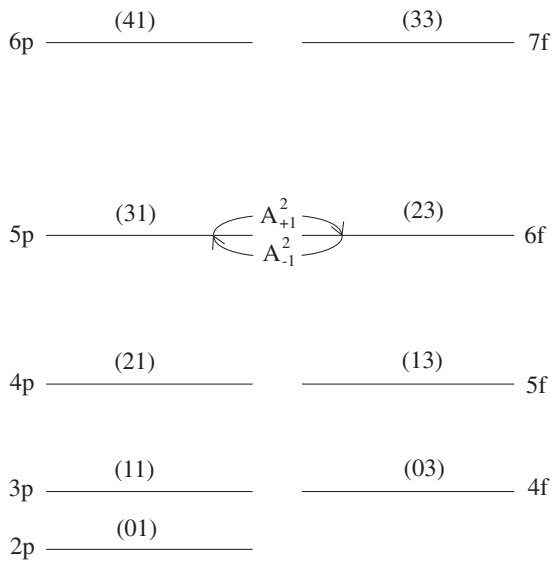

Figure 3. Simultaneous degeneracy between the 2D-CHA p and f states at $\rho_c = 3.75$ and action of the operators A^2_{+1} and A^2_{-1} performing the transformation among them.

A^2_{+1} is the operator decreasing the number of the nodes of the 2D-CHA radial wavefunction by 1, and A^2_{-1} is the operator increasing that number by 1; in other words they are radial node annihilating and creating operators. When the states with negative l values are considered, then these operators act mutually inversely: A^2_{+1} is angular momentum lowering and A^2_{-1} is angular momentum raising operators changing the angular momentum by two units. Simultaneous degeneracy between the np and $(n + 1, \mathrm{f})$ states with $n \geqslant 3$, when the confinement radius is given by the value of the only node of the radial wavefunction of the unconfined 2D hydrogen atom 3p state is illustrated in figure 3. In this display, the spectroscopic notations of the levels are given together with alternative labelling in terms of the radial and magnetic quantum numbers starting from below as (01); (11), (03); (21), (13); (31), (23); (41), (33). This was done with the aim of pictorial understanding of actions of operators $A^2_{\pm}$ which are mentioned above.

It is evident from (26), table 6 and figure 3 that the lowest-laying state with the quantum number l cannot be transformed into any state with the quantum number $l + 2$ under the action of the operator A^2_{+1} and its energy has a specific value given by the energy of the unconfined 2D hydrogen atom state with the same l and $n = l + 2$,

$$E = -\frac{1}{2\left(l + \frac{3}{2}\right)^2}. \tag{27}$$

This result can be corroborated by finding the first-order derivative of the function h_{+1} at the confinement radius value given by (23) and for E given by (27)

$$\left(\frac{\mathrm{d}h_{+1}}{\mathrm{d}\rho}\right)_{\rho=\rho_c} = \left[1 - \frac{4(l+1)}{2l+3} - \frac{E(2l+1)(2l+3)}{2}\right] \times \left(\frac{\mathrm{d}R_{nl}}{\mathrm{d}\rho}\right)_{\rho=\rho_c} = 0, \tag{28}$$

Table 6. Simultaneous degeneracy of the pairs of the 2D-CHA states $[(nl), (n+1, l+2)]$ with $l = 0, \ldots, 3$ and $n = l+2, l+3, \ldots, l+7$ at the values of the confinement radius given by (23).

$\rho_c = 0.75$			$\rho_c = 3.75$		
n	E_{ns}	$E_{n+1,d}$	n	E_{np}	$E_{n+1,f}$
1	−0.222 22		2	−0.080 00	
2	21.135 03	21.135 03	3	1.023 86	1.023 86
3	60.076 94	60.076 94	4	2.865 66	2.865 66
4	116.714 24	116.714 24	5	5.431 25	5.431 25
5	190.983 16	190.983 16	6	8.711 87	8.711 87
6	282.852 94	282.852 94	7	12.703 13	12.703 13
7	392.306 75	392.306 75	8	17.402 51	17.402 51
$\rho_c = 8.75$			$\rho_c = 15.75$		
n	E_{nd}	$E_{n+1,g}$	n	E_{nf}	$E_{n+1,h}$
3	−0.040 82		4	−0.024 69	
4	0.204 44	0.204 44	5	0.063 49	0.063 49
5	0.591 24	0.591 24	6	0.197 09	0.197 09
6	1.114 19	1.114 19	7	0.373 71	0.373 71
7	1.770 58	1.770 58	8	0.592 20	0.592 20
8	2.558 99	2.558 99	9	0.851 94	0.851 94
9	3.478 58	3.478 58	10	1.152 56	1.152 56

and concluding that

$$h_{+1} \equiv 0 \tag{29}$$

since both the function h_{+1} and its first-order derivative have the zero values at the boundary. This is also the reason for the restriction on the principal quantum number given by the inequality $n \geqslant l + 2$ in (26).

5. Summary and concluding remarks

In this paper, we investigated the energy spectrum of the 2D-CHA using the Numerov–Cooley method for the numerical integration of the radial Schrödinger equation. This finite difference method enabled us to compute the energy values of the ground and excited states with high numerical accuracy and in satisfactory agreement with those reported in the literature. The dipole polarizability for the ground state calculated using our method is found to be in excellent agreement with the other available data. We have shown that with the choice of confinement radius, ρ_c, as equal to the location of the radial node of the unconfined atom state $(l + 2, l)$, all the successive pairs of the confined (nl) and $(n + 1, l + 2)$ states, such that $n \geqslant l + 2$, become degenerate. Although the Coulomb degeneracy, characteristic for the unconfined 2D hydrogen atom states is removed, some kind of degeneracy is still preserved due to the fact that there are the operators A^2_{+1} and A^2_{-1} commuting with the 2D-CHA Hamiltonian performing transformation among the states, as indicated above, when the confining radius has the specific value (23). In other words, the set of mutually degenerated states (nl) and $(n + 1, l + 2)$ with $n \geqslant l+2$ for the ρ_c value given by (23) forms the subspace in the Hilbert space of the considered quantum system which is the domain of the operators A^2_{+1} and A^2_{-1}.

It is interesting to note here that simple quantum systems, such as the hydrogen atom and isotropic harmonic oscillator, confined inside the radially symmetric boundary in both two and three dimensions, exhibit some peculiarities in their eigenspectra. These properties appear when the confining radius is determined by the value of the only zero in the radial wavefunction of the state with the radial quantum number equal to 1 of their unconfined (free) counterparts. Thus, when hydrogen atoms confined in 3D [21, 28, 29] and 2D are considered, simultaneous degeneracy among the corresponding states still exists, unlike the confined 2D harmonic oscillator for which the equally energy spacing of exactly 2 h.o. units among the number of corresponding states is observed [30]. The corresponding behaviour of the confined 3D harmonic oscillator is currently being pursued.

Acknowledgments

We are grateful to the referees for their constructive suggestions that helped us to make the presentation clearer.

References

[1] Michels A, De Boer J and Bijl A 1937 *Physica* **4** 981
[2] Jaskólski W 1996 *Phys. Rep.* **271** 1
[3] Dolmatov V K, Baltenkov A S, Connerade J-P and Manson S T 2004 *Rad. Phys. Chem.* **70** 417
[4] Chang L L, Esaki L and Tsu R 1974 *Appl. Phys. Lett.* **24** 593
[5] Dingle R, Gossard A C and Weigmann W 1974 *Phys. Rev. Lett.* **33** 827
[6] Schmelcher P and Schweizer W (ed) 2002 *Atoms and Molecules in Strong External Fields* (New York: Kluwer) chapter 36
[7] Klitzing K, Dorda G and Pepper M 1980 *Phys. Rev. Lett.* **45** 494
[8] Tsui D, Stormer H L and Gossard A C 1982 *Phys. Rev. Lett.* **48** 1559
[9] Katayama M, Williams R S, Kato M, Nomura E and Aono M 1991 *Phys. Rev. Lett.* **66** 2762

[10] Vasilyev S, Järvinen J, Safonov A I and Jaakkola S 2004 *Phys. Rev.* A **69** 023610
[11] Kubo O, Ryu J T, Katayama M and Oura K 2004 *Phys. Rev.* A **69** 045406
[12] Aquino N, Campoy G and Flores-Riveros A 2005 *Int. J. Quantum Chem.* **103** 267
[13] Chaos-Cador L and Ley-Koo E 2005 *Int. J. Quantum Chem.* **103** 369
[14] Yang X L, Guo S H, Chan F T, Wong K W and Ching W Y 1991 *Phys. Rev.* A **43** 1186
[15] Numerov B 1933 *Publs. Observatoire Central. Astrophys. Russ.* **2** 188
[16] Cooley J W 1961 *Math. Comp.* **15** 363
[17] Jensen P 1983 *Comp. Phys. Rep.* **1** 1
[18] Richtmyer R D 1978 *Principles of Advanced Mathematical Physics* Vol 1 (New York: Springer)
[19] Arteca G A, Fernández F M and Castro E A 1984 *J. Chem. Phys.* **80** 1569
[20] Abramowitz M and Stegun I A (ed) 1972 *Handbook of Mathematical Functions* (New York: Dover)
[21] Scherbinin A V, Pupyshev V I and Ermilov A Yu 1997 *Physics of Clusters* (Singapore: World Scientific) p 273
[22] Guimarães M N and Prudente F V 2005 *J. Phys. B: At. Mol. Opt. Phys.* **38** 2811
[23] Burrows B L and Cohen M 2005 *Phys. Rev.* A **72** 032508
[24] Sahoo S and Ho Y K 2004 *Phys. Rev.* B **69** 165323
[25] Liu Y F, Huo W J and Zeng J Y 1998 *Phys. Rev.* A **58** 862
[26] Wu Z B and Zeng J Y 2000 *Phys. Rev.* A **62** 32509
[27] Reed M and Simon B 1978 *Methods of Modern Mathematical Physics. IV: Analysis of Operators* (New York: Academic)
[28] Pupyshev V I and Scherbinin A V 1998 *Chem. Phys. Lett.* **295** 217
[29] Pupyshev V I and Scherbinin A V 2002 *Phys. Lett.* A **299** 371
[30] Stevanović Lj and Sen K D 2008 *J. Phys. A: Math. Theor.* **41** 265203